Comparison of Flux Regulation and Follow-B approach for enabling Magnetic Resonance (MR) Imaging in Powered magnets

Rohan R. Shah

School of Electrical Engineering and Computer Science
The Pennsylvania State University, University Park, PA 16802

Abstract

Clinical magnetic resonance (MR) imaging systems typically operate at 1.5 Tesla using low-temperature superconducting (LTS) magnets that provide a spatially uniform and temporally constant magnetic field. The downside of LTS magnets include high initial cost, large physical size, and the expense of replenishing cryogens. Development of compact and cryogen-free magnet systems could lead to the widespread use of MR systems in physician's offices. Replacing LTS magnets with powered or permanent magnets presents an engineering challenge as the resulting magnetic fields are not temporally constant. This research compares the flux regulation and Follow-B approach on MR imaging using the scalar performance metric of structural similarity (SSIM). This study provides a benchmark for designing flux regulation systems by indicating the required attenuation of field fluctuations and explains why Follow-B approach is not efficient to enable MR imaging using powered magnets.

1. Introduction

The vast majority of clinical Magnetic Resonance (MR) imaging systems use 1.5 T low-temperature superconducting (LTS) self-persistent magnets. These magnets are well-suited for generating images as they yield a spatially uniform and nearly constant field. These desirable attributes come at an expense. LTS magnets are large, expensive, and require periodic replenishment of cryogens. As a result, MRI systems are confined to hospitals and clinics. It may be possible to overcome these limitations using either permanent or powered magnets [1].

Another disadvantage of LTS magnets is that their maximum field strength is limited to about 23 T. Increasing the field beyond this value is useful in research applications including MR spectroscopy and high resolution MR imaging. As the field strength increases, the chemical shift resolution and signal-to-noise ratio (SNR) increase, while quadrupolar line broadening in solids decreases [2]. While powered magnets provide continuous fields far larger than attainable in self-persistent superconducting magnets, temporal magnetic field fluctuations due to both the power supply ripple and variations in cooling water temperature and flow rate currently render these magnets unsuitable for both spectroscopy and imaging [3].

An earlier study showed that temporal field fluctuations may be significantly attenuated using feedback control [4]. For example, the flux regulator reduces the 60 Hz component in a 25 T, 16 MW resistive magnet by more than 60 dB. The central question of this study is whether or not the Follow-B approach is better than flux-regulation to enable MR imaging in powered

magnets. The second objective is to determine whether Follow-B can allow MR imaging in powered magnets.

Section 2 first shows the baseline MR images acquired in a self-persistent LTS magnet that will be corrupted with the field fluctuations recorded in a powered magnet and pure sinusoids, to study flux regulation and Follow-B respectively. This section also shows the method for artificially inducing the temporal field fluctuations and introduces the structural similarity index metric and Follow-B approach. Section 3 describes the specific simulations performed to study flux regulation and Follow-B compensation method. Section 4 presents and discusses the simulation results, while section 5 states the conclusions drawn from this work. In short, the existing flux regulation system [4] enables MR imaging in powered magnets with additional attenuation while Follow-B is efficient only for certain level of frequencies. The results of this work motivate and guide further improvements in the flux regulation system reported in [4] and discourages the use of Follow-B in MR Imaging.

2. Magnetic Resonance Imaging

MR Images acquired using a Self-Persistent LTS Magnet

This study uses the public domain two-dimensional axial head image shown in Figure 1 for flux regulation and a mouse brain image shown in figure 2 for Follow-B approach. The proton density image (axial head) is acquired with a 1.5 T General Electric MR system [5] while the mouse brain image is acquired with an 11.75-Tesla LTS magnet and Bruker Avance Console. Figure 3 shows the fast spin echo sequence [6] for acquiring the both images while Table 1 and 2 lists the pulse parameters for spin echo sequences for figure 1 and 2 respectively.

Figure 1. Axial head view using proton density weighting

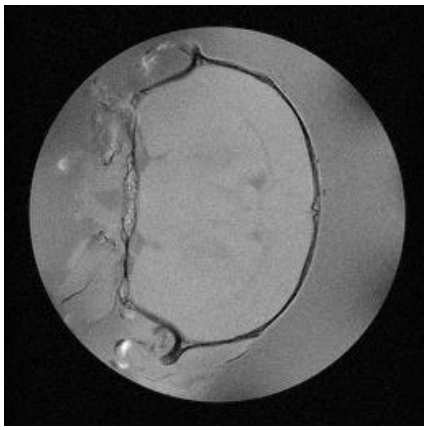

Figure 2. Mouse brain image using

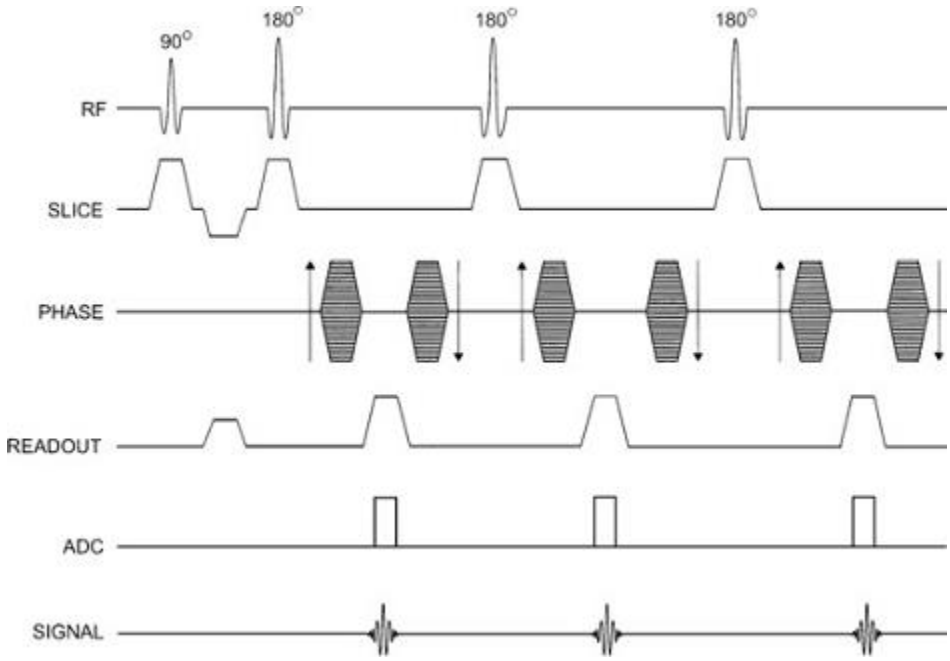

Figure 3. Fast spin echo imaging sequence [7]

Parameter	Value	Units
Field Strength	1.5	T
Echo Time	22	Ms
Repetition Time	2.3	S
Pixel Bandwidth	31.25	kHz
Echo Train Length	8	
Phase Encoding Steps	256	
Sample Points per Echo	256	

Table 1. Parameters for the pulse sequence used for axial head image

Parameter	Value	Units
Field Strength	11.75	T
Echo Time	8.5	Ms
Repetition Time	1.5	S
Pixel Bandwidth	394.57	Hz
Echo Train Length	30	
Phase Encoding Steps	256	
Sample Points per Echo	256	

Table 2. Parameters for the pulse sequence used for mouse brain image

Modeling the field fluctuations

In the absence of temporal field fluctuations, the i^{th} spin echo generated by the pulse sequence in Figure 3 is represented as

$$s_i(t) \propto \iint_{x,y} \rho(x,y) e^{-j\gamma G_y \tau_{pe} y} e^{-j\gamma G_x t x} dx dy, \quad (1)$$

where $\rho(x,y)$ is the proton density, γ is the gyromagnetic ratio, G_y is the phase encoding gradient, τ_{pe} is the duration of the phase encoding gradient, and G_x is the readout gradient [8]. In this expression, the center of the first 90˚ pulse defines t = 0.

Temporal field fluctuations primarily affect the spin echo-phase [3,4]. Assuming that the temporal field fluctuations are spatially uniform, the i^{th} spin echo signal in the presence of spatially uniform magnetic field fluctuations $B_f(t)$ is expressed as

$$s_{i,f}(t) = s_i(t) e^{-j\gamma \int_0^t B_f(\tau) I_{se}(\tau) d\tau}, \quad (2)$$

where $I_{se}(t)$ is an indicator function that accounts for phase reversals induced by the 180˚ pulses that are separated by the echo time T_E. For a constant field perturbation B_f, the indicator function guarantees that $s_{i,f}(t) = s_i(t)$ at the center of each spin echo. The indicator function is a periodic square-wave with period $2T_E$ and amplitude ±1. At the center of the first 90˚ pulse, the value of $I_{se}(t)$ is -1, and switches to +1 at the center of the first 180˚ pulse.

This study uses temporal field fluctuations recorded in a powered magnet and monochromatic fluctuations. The recorded field fluctuations were obtained using the Keck resistive magnet operating at 25 T over a five-minute window using a 17 kHz sample rate [4]. The dashed red curve in Figure 4 shows the spectra of the uncompensated field fluctuations. The spectra reveal large peaks at harmonics of the power supply ripple. The largest component, located at 60 Hz, has an amplitude of approximately 200 mG rms. Using the flux regulation system, the 60 Hz component is reduced by more than 60 dB as shown by the blue curve.

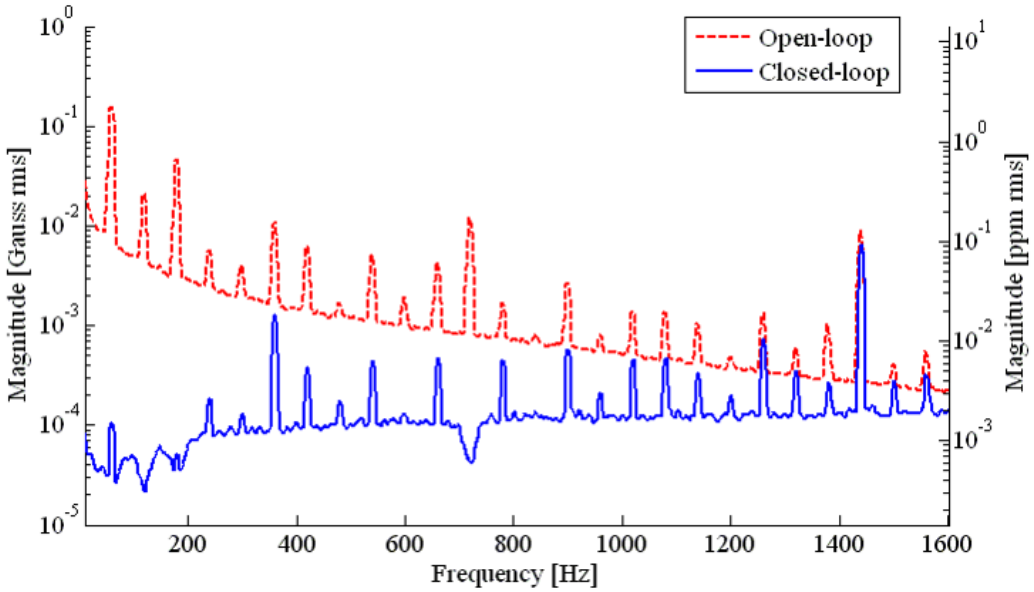

Figure 4. Field fluctuation spectra in the Keck resistive magnet operating at 25 T, with (blue curve) and without (red curve) flux regulation [4]

Image Quality Metric - SSIM

The structural similarity index (SSIM) mimics human perception and judgement by comparing local patterns of pixel intensities that have been normalized for luminance and contrast [9]. Figure 4 shows a block diagram representation of the algorithm for computing the metric J_{SSIM}, which takes on values between unity, when the images are identical, and zero, when the images are uncorrelated. SSIM metric is determined using MATLAB function ssim.

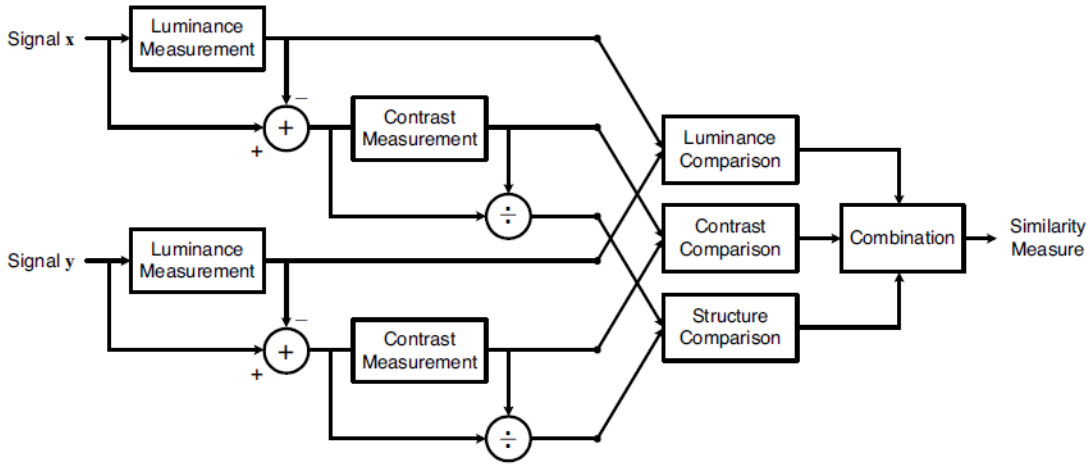

Figure 5. Diagram of the structural similarity (SSIM) measurement system [9]

Follow-B

Follow-B approach is one of the method for compensating field fluctuations. This approach measures the resonance frequency right before the application of pulse sequence by observing the

precision frequency of nuclei and based on this frequency, field strength is approximated. Imaging sequence is immediately applied using measured magnetic field strength. This information is then used to set and receive frequency of the MR image and this way the field drifts the … The disadvantage of this method is that it assumes field remains constant. The idea of this study is to determine how this approach works in presence of field fluctuations.

3. Simulation Description

Two sets of simulation experiments are designed to answer the central research question, does the flux regulation and Follow-B both provide sufficient attenuation of field fluctuations to allow MR imaging in powered magnets?

Flux Regulation

In the first set of simulation experiments, the recorded Keck noise is incorporated into the spin echo data for human brain image using Equation (2). As the sample rate of the recorded noise is 17 kHz, while the pixel bandwidth of the MR acquisition is 32.5 kHz, the recorded Keck measurements are interpolated to yield an effective sample rate of 32.5 kHz. Three images are generated. The first and second image use the recorded Keck noise without and with flux regulation. To generate the third image, the compensated field fluctuations are attenuated by an additional 40 dB to predict the performance of an improved flux regulation scheme.

Follow-B

The second set of simulation experiments uses the following monochromatic field fluctuation:

$$B_f(t) = 0.001\cos(2\pi f t)\ [\mathrm{G}], \tag{4}$$

for corrupting mouse brain image to study the efficiency of Follow-B approach. For this set of simulations, eight images are generated, where first four images are corrupted with the monochromatic field fluctuation from equation (4) with 3 Hz, 0.3 Hz, 0.03 Hz, and 0.003 Hz frequencies. And next four images are generated by attenuating the field fluctuation using compensation field, where compensation field is the average of first 200 μs before π/2 pulse of the corresponding spin-echo sequence, as represented by equation (5):

$$< B_d >_i = -\frac{1}{T_o}\int_{t_i}^{t_{i+200}} B_f(\tau)\,.\,d\tau. \tag{5}$$

Figure (6) shows the spin-echo sequences for Follow-B approach after applying compensation field:

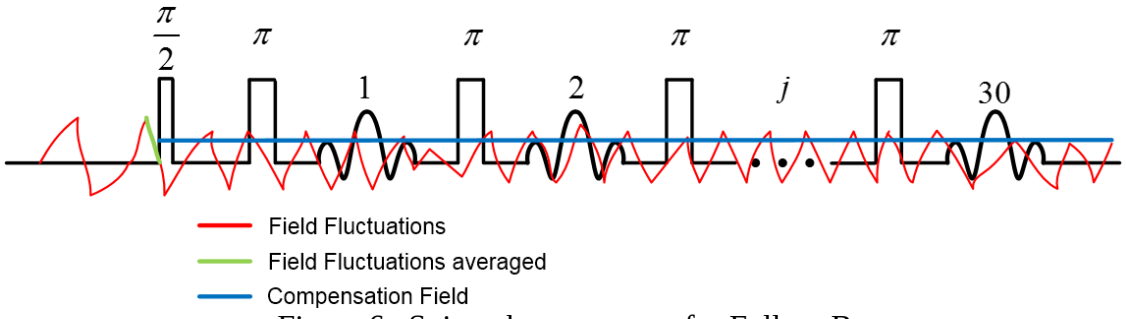

Figure 6. Spin-echo sequences for Follow-B

4. Simulation Results and Discussion

Figure 7 shows the predicted MR images obtained in the presence of magnetic field fluctuations recorded in the Keck powered magnet. As a reference, Figure 7(a) shows the original MR image acquired in a self-persistent 1.5 T superconducting magnet. The image in Figure 7(b) reveals the effect of the uncompensated field fluctuations on the image. Using a flux regulator [4] to reduce temporal field fluctuations results in the image shown in Figure 7(c). Using an improved flux regulator that provides an additional 40 dB of attenuation yields the image in Figure 7(d). The image quality metric J_{SSIM} is shown for each of these images in Table 2.

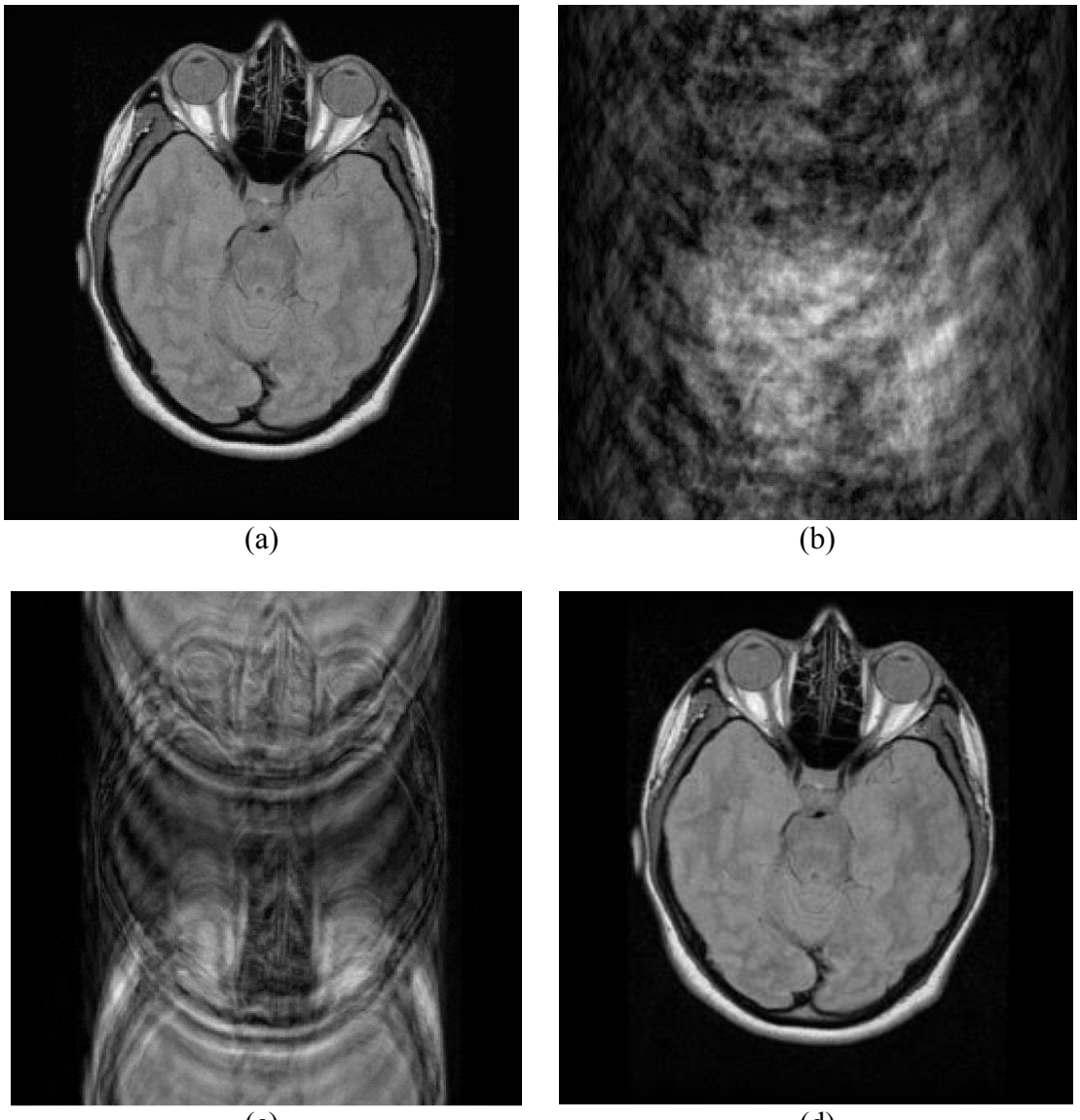

(a) (b)

(c) (d)

Figure 7. (a) No field fluctuations, (b) uncompensated field fluctuations, (c) compensated field fluctuations, and (d) compensated field fluctuations with an additional 40 dB of attenuation

Figure 7(b) clearly illustrates the challenge of generating a MR image in the presence of temporal field fluctuations as they severely distort the image. Comparing Figures 7(a) through 7(d) answers the one of the questions posed by this study. The existing flux regulator is not sufficient, but an additional 40dB of attenuation as shown in Figure 7(d) is sufficient enough to attenuate the temporal field fluctuations for a powered magnet to produce a MR image of clinical value.

	No Fluctuations	Uncompensated Fluctuations	Compensated Fluctuations	Compensated Fluctuations with 40 dB Attenuation
J_{SSIM}	1	6.03×10^{-3}	4.203×10^{-2}	9.744×10^{-1}

Table 3. SSIM metric values for flux regulated simulated images in Figure 7

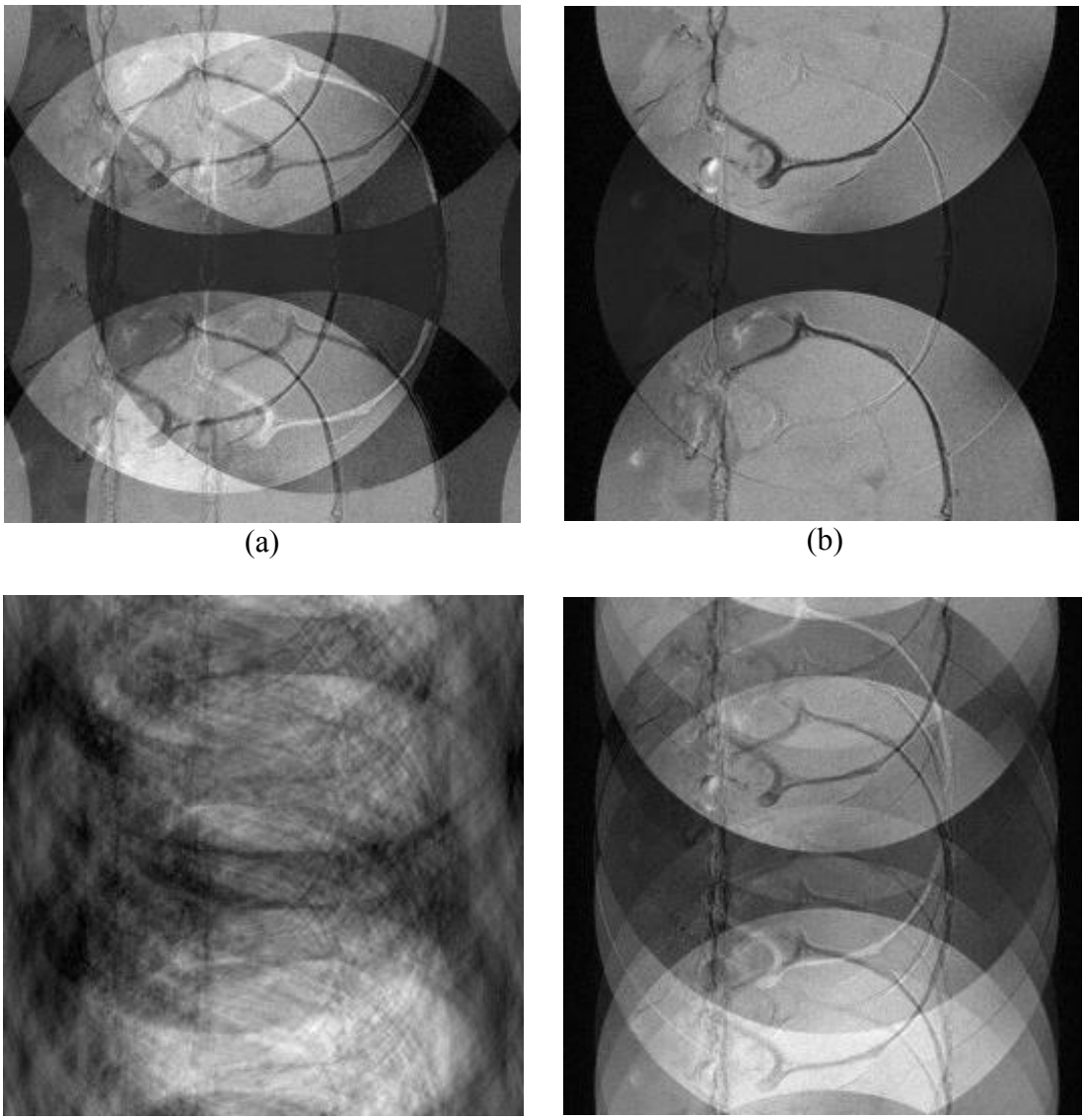

(a) (b)

(c) (d)

Figure 8. (a) 3 Hz monochromatic field fluctuations, (b) Follow-B compensated for 3 Hz monochromatic field fluctuations, (c) 0.3 Hz monochromatic field fluctuations, and (d) Follow-B compensated for 0.3 Hz monochromatic field fluctuations

Figures 8 and 9 represent the corrupted MR images obtained using monochromatic field fluctuations represented by equation (4). Figure 8(a) shows the MR image corrupted using 3 Hz monochromatic field fluctuation and Figure 8(b) represents the attenuation of the same field fluctuation using Follow-B compensation field from equation (5). Similarly, Figures 8(c), 9(a), and 9(c) show the MR image obtained in presence of 0.3 Hz, 0.03 Hz, and 0.003 Hz monochromatic field fluctuations, respectively, while Figures 8(d), 9(b), and 9(d) illustrate Follow-B compensated MR image for corresponding frequencies. Table 4 represents the J_{SSIM} metric value for each images in Figures 8 and 9 and the uncorrupted image from Figure (2).

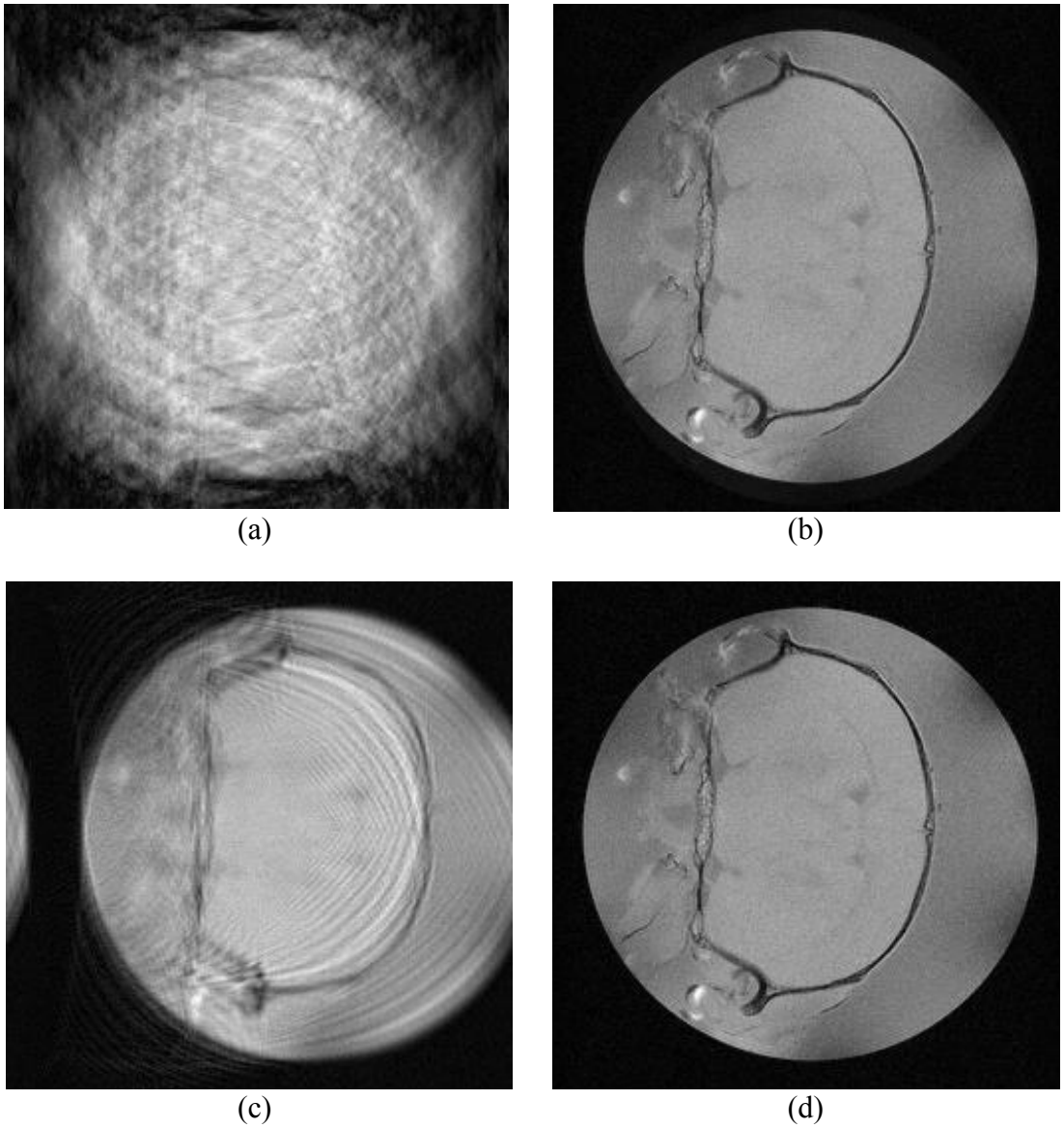

(a) (b)

(c) (d)

Figure 9. (a) 0.03 Hz monochromatic field fluctuations, (b) Follow-B compensated for 0.03 Hz monochromatic field fluctuations, (c) 0.003 Hz monochromatic field fluctuations, and (d) Follow-B compensated for 0.003 Hz monochromatic field fluctuations

Frequency	J_{SSIM}	
	Monochromatic Fluctuations (Hz)	Compensated Fluctuations
No fluctuations (original image)	1	1
3 Hz	1.64×10^{-1}	3.099×10^{-1}
0.3 Hz	1.659×10^{-1}	2.713×10^{-1}
0.03 Hz	2.135×10^{-1}	9.81×10^{-1}
0.003 Hz	2.93×10^{-1}	9.993×10^{-1}

Table 4: J_{SSIM} metric values for Follow-B simulated images in Figures 8 and 9

After comparing Figures 8 (a) through (d) and Figures 9 (a) through (d), it is evident that the Follow-B technique is efficient only for lower frequencies monochromatic field fluctuations of the order of 10^{-2} Hz or less. Figures 8 (b) and (d) clearly has replicas in vertical direction and those images were corrupted using 3 Hz and 0.3 Hz respectively. While Figures 9 (b) and (d) are identical to Figure (2), which can also be inferred from table 4, where Follow-B compensated images with 0.03 Hz and 0.003 Hz field fluctuations has J_{SSIM} metric values close to 1.

5. Conclusions

Two conclusions emerge from this work. First, the existing flux regulator described in [4] is not sufficient, additional 40 dB of attenuation is required to allow MR imaging in powered magnets. Second, Follow-B technique is efficient only for lower frequencies of field fluctuations, and therefore, should not be used for MR imaging in presence of fast field fluctuations.

Flux regulation provides a means for improving the quality of MR images acquired with magnets that do not possess the field stability of LTS magnets. In addition to high field magnets, such as the 30 Tesla series connected hybrid magnet under development at the National High Magnetic Field Laboratory, flux regulation facilitates the use of low-cost, low-field powered and permanent magnets for MRI.

Acknowledgements

I am thankful for contributions from Ph.D candidate Xinxing Meng and Dr. Jeffrey Schiano from The Pennsylvania State University. This work was supported by the College of Engineering Research Initiative at The Pennsylvania State University and the National High Magnetic Field Laboratory which is supported by National Science Foundation Cooperative Agreement No. DMR-1157490, the State of Florida, and the U.S. Department of Energy.

References

[1]. T. Miyamoto, H. Sakurai, H. Takabayashi and M. Aoki, 'A development of a permanent magnet assembly for MRI devices using Nd-Fe-B material', *IEEE Transactions on Magnetics*, vol. 25, no. 5, pp. 3907-3909, 1989.

[2]. H. Schneider-Muntau, 'High field NMR magnets', *Solid State Nuclear Magnetic Resonance*, vol. 9, no. 1, pp. 61-71, 1997.

[3]. E. Sigmund, E. Calder, G. Thomas, V. Mitrović, H. Bachman, W. Halperin, P. Kuhns and A. Reyes, 'NMR Phase Noise in Bitter Magnets', *Journal of Magnetic Resonance*, vol. 148, no. 2, pp. 309-313, 2001.
[4]. M. Li, J. Schiano, J. Samra, K. Shetty and W. Brey, 'Reduction of magnetic field fluctuations in powered magnets for NMR using inductive measurements and sampled-data feedback control', *Journal of Magnetic Resonance*, vol. 212, no. 2, pp. 254-264, 2011.
[5]. J. Mather, 'DICOM Example Files', *The MATLAB Digest*, vol. 10, no. 6, 2002.
[6]. J. Hennig and H. Friedburg, 'Clinical applications and methodological developments of the RARE technique', *Magnetic Resonance Imaging*, vol. 6, no. 4, pp. 391-395, 1988.
[7]. Bitc.bme.emory.edu, 2015. [Online]. Available: http://bitc.bme.emory.edu/images/fse_pt_1.jpg. [Accessed: 21- Jul- 2015].
[8]. E. Haacke, *Magnetic resonance imaging*. New York: Wiley, 1999.
[9]. Z. Wang, A. Bovik, H. Sheikh and E. Simoncelli, 'Image Quality Assessment: From Error Visibility to Structural Similarity', *IEEE Transactions on Image Processing*, vol. 13, no. 4, pp. 600-612, 2004.